

Journal of Nanophotonics

SPIDigitalLibrary.org/jnp

Anisotropy in polyetheretherketone films

Jasmin Althaus
Hans Deyhle
Oliver Bunk
Per Magnus Kristiansen
Bert Müller

Anisotropy in polyetheretherketone films

Jasmin Althaus,^a Hans Deyhle,^{a,b} Oliver Bunk,^b Per Magnus Kristiansen,^c
and Bert Müller^a

^aUniversity of Basel, Biomaterials Science Center, c/o University Hospital Basel,
4031 Basel, Switzerland
bert.mueller@unibas.ch

^bPaul Scherrer Institute, Swiss Light Source, 5232 Villigen, Switzerland

^cUniversity of Applied Sciences and Arts Northwestern Switzerland, Institutes of Polymer
Engineering & Polymer Nanotechnology, 5210 Windisch, Switzerland

Abstract. Optical measurements reveal the preferential orientation of nanostructures within polymer films, which results from the fabrication process including mechanical and thermal treatments. As the wavelength of the incident light is generally much larger than the characteristic dimensions of the molecular arrangement in semi-crystalline or amorphous polymers, the optical signal originates not directly from the nanostructure of the polymers. Linear dichroism measurements were correlated with synchrotron radiation-based x-ray scattering data on commercially available polyetheretherketone (PEEK) thin films (12 to 50 μm). Annealing changed the structure of amorphous films to semi-crystalline ones associated with the measured linear dichroism. The intensity of the measured anisotropic signal depended on the film thickness. While for wavelengths between 450 and 1100 nm the transmission was higher when the polarizer was parallel to the machine direction, for larger wavelengths maximum transmission was observed with the polarizer perpendicular to the machine direction indicating excitations parallel and perpendicular to the PEEK molecule axis, respectively. Annealing PEEK films at temperatures between 160 and 240°C decreased the transmission at 540 nm by a factor of two, whereas the anisotropy remained constant. x-ray scattering revealed strongest anisotropy for a periodicity of 15 nm in the machine direction of the cast film extrusion process. The long-range order of amorphous and semi-crystalline entities can explain the x-ray scattering data and the related optical anisotropy of casted PEEK films. © 2012 Society of Photo-Optical Instrumentation Engineers (SPIE). [DOI: [10.1117/1.JNP.6.063510](https://doi.org/10.1117/1.JNP.6.063510)]

Keywords: anisotropy; polyetheretherketone; x-ray scattering; synchrotron radiation; long-range order.

Paper 12014 received Feb. 16, 2012; revised manuscript received Mar. 29, 2012; accepted for publication Apr. 2, 2012; published online Jul. 2, 2012.

1 Introduction

As a result of the fabrication process, polymer films often exhibit an optical anisotropy.¹⁻⁵ This anisotropy can simply be quantified from transmission measurements of the film between crossed polarizers at wavelengths from ultraviolet to infrared.^{1,6} Usually, these wavelengths from 200 to 2,500 nm are much larger than the structures within the nano-crystalline or even amorphous polymers and the origin of the detected optical anisotropy cannot be resolved.

Polyetheretherketone (PEEK) is a high-performance, thermoplastic polymer used in a number of applications including medical implants.⁷ Due to its structure and related inertness, PEEK is biocompatible and used, e.g., for pacemaker housings⁸ and load-bearing spine implants.⁷ Very recently, it has been demonstrated that dedicated plasma treatments of PEEK films result in nanostructures on the surface with feature sizes depending on the choice of process gas, applied power and treatment duration.⁹ By tailoring the nanostructure of implant surfaces, tissue integration might be accomplished, which broadens the fields of application for PEEK. As human tissues usually exhibit an anisotropic nanostructure,¹⁰ PEEK implants should preferably also

display anisotropy at these length scales. Appropriate methods to characterize the oriented structure and anisotropy properties of PEEK are necessary.

In this article we demonstrate that micrometer-thin, commercially available PEEK films show an optical anisotropy, represented by the linear dichroism, which relates to nanostructures revealed by means of x-ray scattering. The combination of small- and wide-angle x-ray scattering should permit the development of a structural model for PEEK that also explains the mechanically and thermally induced transitions from amorphous to (partially) crystalline states in PEEK films. In order to differentiate between surface and bulk phenomena, specimens of different thickness were incorporated in the study.

2 Materials and Methods

2.1 Materials and Preparation

Commercially available amorphous and semi-crystalline PEEK films (APTIV™ 2000 and 1000 series, respectively, Victrex Europa GmbH, Hofheim, Germany) of 12, 25, and 50 μm thickness were marked to identify machine and transverse directions with respect to the extrusion process. They were subjected to annealing under pressure. For this purpose, the films were placed between two polished, 500 μm thick, 4-inch Si(100) wafers (Si-Mat, Kaufenring, Germany) in a precision hot press (HEX03, JENOPTIK Mikrotechnik GmbH, Jena, Germany) at temperatures between 160 and 240°C with a pressure of 12.3 MPa for a period of 10 min and subsequently cooled down with an average rate of 0.26 K/min.

2.2 Optical Measurements

Transmission spectra of the PEEK films were recorded with a spectrometer (Lambda 19, Perkin Elmer, Überlingen, Germany) covering the wavelength range between 200 and 2,500 nm. The system was equipped with a rotatable polarizer (analyzer). For optical anisotropy measurements, PEEK films were mounted on a rotation table, and rotated in steps of 10 degrees. The angle of zero degree corresponded to the machine direction. The 0.7 mm-thick polarizer film HN 32 (SreenLab, Elmshorn, Germany) was made of polyvinyl alcohol.

2.3 x-Ray Scattering

The small- and wide-angle x-ray scattering (SAXS/WAXS) data were recorded at the cSAXS beamline of the Swiss Light Source (Paul Scherrer Institut, Villigen, Switzerland) using a two-dimensional (2-D) scanning setup.¹¹ The measurements were performed at a photon energy of 8.7 keV, corresponding to a wavelength of $\lambda = 1.43 \text{ \AA}$. The films were mounted over apertures of an aluminum frame. This frame was moved by a translation stage in two orthogonal directions. Scattering patterns were recorded by a PILATUS 2M detector¹² with a pixel size of 172 μm . The exposure time was set to 0.5 s per frame. The data were averaged over 100 frames recorded in a line scan with a step size of 5 μm . The specimen-detector distance, which corresponded to 2.17 m, was calculated from the first scattering order of a silver behenate powder. WAXS measurements with 2 s exposure time per frame were performed at a photon energy of 11.2 keV ($\lambda = 1.11 \text{ \AA}$) and a detector distance of 0.578 m. Data evaluation was performed with dedicated self-written MATLAB® (2010b, TheMathWorks, Natick, USA) code.

3 Results

3.1 Optical Measurements

To characterize the potentially anisotropic structure of annealed micrometer-thin PEEK films, a transmission scan varying the wavelength from ultraviolet to infrared was performed. As shown in Fig. 1(b), the 50 μm -thin APTIV™ 2000 PEEK film annealed at 160°C, revealed differences in absorbance parallel and perpendicular to the machine direction. At wavelengths between 400

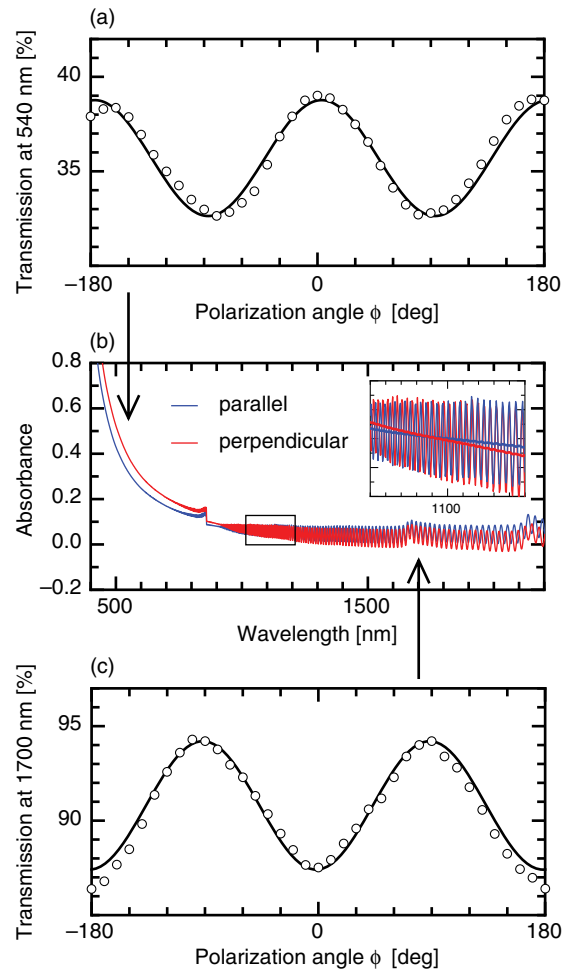


Fig. 1 Anisotropic characteristics of a 50- μm APTIV™ 2000 PEEK film, annealed at 160°C, in a polarizer setup. (b) The middle graph shows the absorbance with the polarizer position parallel and perpendicular to machine direction. Maximum anisotropy is reached at approximately 540 nm and a phase shift occurs around 1100 nm (see inset). The inset shows in addition to the absorbance the values averaged along ± 100 nm. (a) At 540 nm, below the phase shift around the maximum of the anisotropy, a 360 deg transmission measurement followed a sinusoidal curve with the transmission maximum in machine direction. (c) At 1700 nm, above the phase shift, the 360 deg rotation resulted in a sinusoidal curve with the transmission maximum in transverse direction.

and 1100 nm, the absorbance was lower when the analyzer was oriented in machine direction. For wavelengths above 1100 nm, the absorbance in machine direction was higher than in transverse direction. This phase shift clearly indicates anisotropic behavior. Note the Fabry-Pérot fringes, that occur in the near infrared range, originate from interferences due to the thin film nature of the PEEK sheets. Optical anisotropy is often identified with linear dichroism.¹³ It is defined as the difference in the absorbance parallel and perpendicular to the molecular axis. The linear dichroism is related to the molecular structure and the interactions of the molecules with the incident electromagnetic waves. Therefore, the PEEK film was further investigated below and above the phase shift at 1100 nm. Below this neutral point [see inset of Fig. 1(b)], the anisotropy reached a maximum at a wavelength of about 540 nm. A characteristic transmission curve, recorded at 540 nm as a function of the rotation angle, is shown in Fig. 1(a). The transmission follows a sinusoidal function with maxima along the machine direction, indicating a preferential alignment of the molecules within the plane of incidence. For the wavelength of 1700 nm [Fig. 1(c)], well above the phase shift wavelength, the sinusoidal function was shifted by 90 deg with respect to the one recorded at 540 nm. The transmission showed maxima in transverse direction. In a control experiment, the amorphous APTIV™ 2000 PEEK films

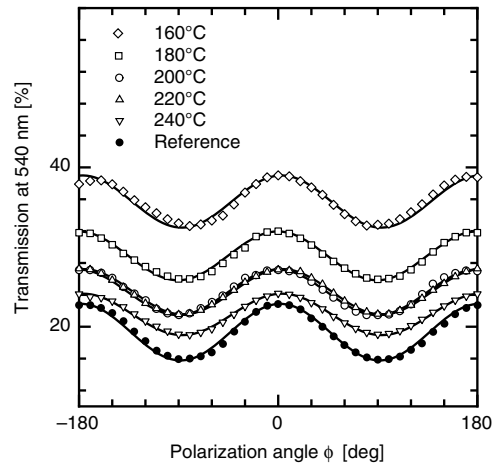


Fig. 2 Transmission at 540 nm of 50 μm APTIV™ 2000 PEEK films subjected to annealing at the temperatures indicated. Reference is a 50 μm -thin APTIV™ 1000 PEEK film. Sinusoidal behavior of the transmission with a maximum in machine direction is observed for all samples including the reference.

(not annealed) did not show any linear anisotropy. These optical measurements confirm the apparent isotropy of the source material prior to the annealing process. In order to investigate this orientation effect in more detail, the anisotropy in absorbance of APTIV™ 2000 PEEK films was studied as a function of the annealing temperature above the glass transition temperature at 143°C. Annealing of 50 μm -thin APTIV™ 2000 PEEK films at temperatures between 160 and 240°C induced similar anisotropy as found in a semi-crystalline APTIV™ 1000 PEEK film of same thickness (Fig. 2). The amplitude of the sinusoidal curves slightly decreased with increasing annealing temperature. Annealing at a temperature of 240°C led to a similar transmission as found for the APTIV™ 1000 PEEK films. The higher annealing temperatures are associated with enhanced crystallinity. This effect decreases the transmission due to light scattering. The annealing supports the molecule alignment into crystallite assemblies detectable as optical anisotropy in the originally amorphous PEEK films. Table 1 quantitatively summarizes the anisotropy by the amplitude and the ratio of transmissions in machine and transverse directions

Table 1 Anisotropy quantification of APTIV™ 1000 and 2000 PEEK films and a polarizer foil HN32 by transmission measurements. The mean transmission τ_M and the amplitude τ_A were derived from fitting the sinusoidal transmission behavior between crossed polarizers at the wavelength of 540 nm. The ratio of transmission measurements in machine and transverse directions τ_{MD}/τ_{TD} characterizes the PEEK film anisotropy.

| Film | $T_{\text{annealing}}$ [°C] | Film thickness [μm] | τ_M [%] | τ_A [%] | τ_{MD}/τ_{TD} |
|----------------|-----------------------------|----------------------------------|----------------|----------------|-----------------------|
| APTIV™ 1000 | | 25 | 35.8 ± 0.1 | 4.0 ± 0.1 | 1.3 ± 0.0 |
| APTIV™ 1000 | | 50 | 19.3 ± 0.1 | 3.6 ± 0.1 | 1.5 ± 0.0 |
| APTIV™ 2000 | | 50 | 18.3 ± 0.1 | 0 | 0 |
| APTIV™ 2000 | 160 | 50 | 35.7 ± 0.1 | 3.2 ± 0.2 | 1.2 ± 0.1 |
| APTIV™ 2000 | 180 | 50 | 28.9 ± 0.1 | 3.0 ± 0.2 | 1.2 ± 0.1 |
| APTIV™ 2000 | 200 | 50 | 24.3 ± 0.1 | 2.9 ± 0.2 | 1.3 ± 0.1 |
| APTIV™ 2000 | 220 | 50 | 24.4 ± 0.1 | 2.9 ± 0.2 | 1.3 ± 0.1 |
| APTIV™ 2000 | 240 | 50 | 21.5 ± 0.1 | 2.6 ± 0.1 | 1.3 ± 0.1 |
| HN32 polarizer | | 700 | 19.4 ± 0.1 | 19.3 ± 0.1 | 552 ± 6 |

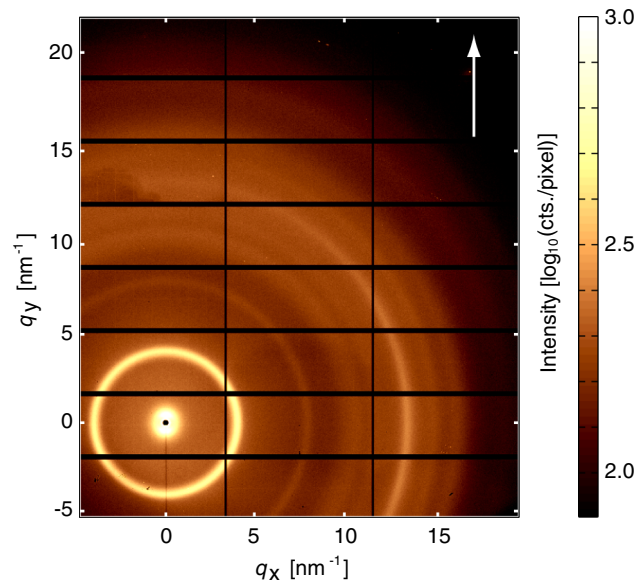


Fig. 3 WAXS pattern of a 50 μm -thin 2000 APTIV™ PEEK film annealed at 160°C for 10 min, featuring the characteristic peaks of PEEK. The most prominent anisotropic ring relates to the (110) plane. The white-colored arrow indicates the machine direction.

calculated from sinusoidal fits for the 25 and 50 μm -thin 2000, annealed and 1000 APTIV™ PEEK films investigated at a wavelength of 540 nm. The transmission ratios rose from 1.19 to 1.27, while the mean transmission decreased from 35.72% to 21.54% when increasing annealing temperatures from 160 to 240°C. A 50 μm -thin APTIV™ 1000 PEEK film showed a transmission of 19.32% and a transmission ratio of 1.45. The 50 μm -thin APTIV™ 2000 PEEK film exhibited low transmission since it had a rough surface on one side, which caused significant light scattering. As a reference, we examined a commercially available linear polarizer film (HN32). In comparison to the PEEK films, we found a transmission ratio of more than 500 for the HN32 polarizer film, stating that the polarization and therefore anisotropy of the PEEK films is fairly weak. The absolute amplitude of the polarizer film, however, was only 4 to 5 times larger.

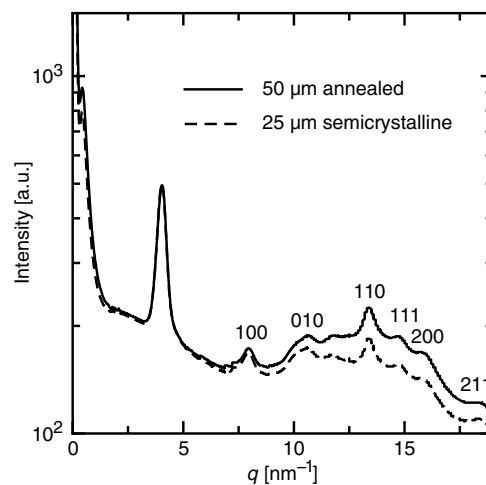


Fig. 4 Radially integrated WAXS intensities (q -plot) of a 25 μm -thin APTIV™ 1000 PEEK film (dashed line) and a 50 μm -thin APTIV™ 2000 PEEK film (solid line) after annealing at 160°C for 10 min. Miller indices are given for peaks of the PEEK unit cell.

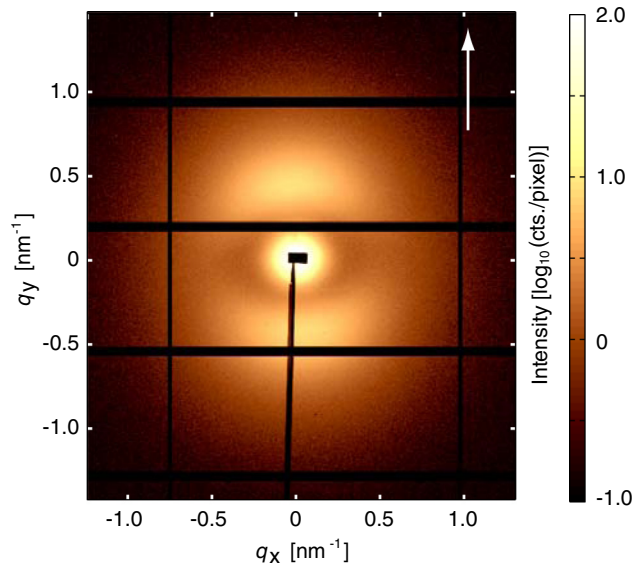


Fig. 5 SAXS pattern of a 50 μm -thin APTIV™ 2000 PEEK film annealed at 160°C for 10 min. The anisotropic scattered intensity distribution with a maximum q -value of 0.43 nm^{-1} indicates preferential long-range order in the machine direction, see white arrow. Data were recorded in a q -range between 0.09 to 3.4 nm^{-1} .

3.2 x-Ray Scattering Measurements Using Synchrotron Radiation

In order to gain more detailed information about the investigated anisotropy of the PEEK films on the molecular scale, WAXS data of the PEEK films were recorded. As shown in Fig. 3, the APTIV™ PEEK films give rise to intensity distributions at well-defined scattering angles of 0.4 nm^{-1} , 4.0 nm^{-1} , 8.0 nm^{-1} , 10.7 nm^{-1} , and 13.4 nm^{-1} , corresponding to feature sizes of 14.66 nm, 1.56 nm, 0.79 nm, 0.59 nm, and 0.47 nm, respectively. Anisotropic sinusoidal intensity modulations along the ring were clearly identified for the features with sizes of 14.66 nm and 0.47 nm, oriented in machine and transverse directions, respectively. The crystallographic unit

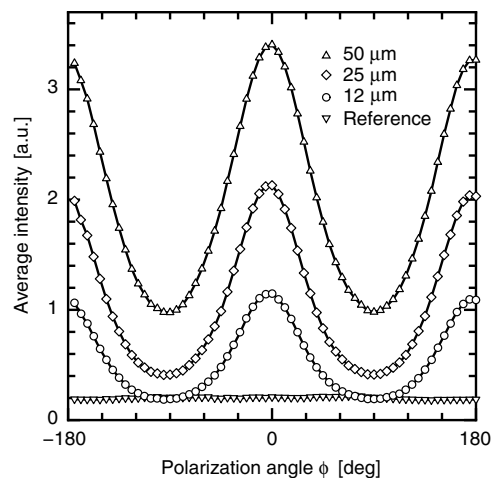


Fig. 6 Azimuthal intensity plot (from 2-D SAXS data integrated over the q -range related to real space periodicities between 5.2 and 22.5 nm) for PEEK films of different film thickness (after annealing to 160°C). A 50 μm -thin amorphous PEEK film is also included as reference, revealing the distinct anisotropy of the scattered intensity in the annealed films. Maxima were found in the machine direction. Their intensity was almost directly proportional to the material thickness while no modulation was found in the amorphous PEEK.

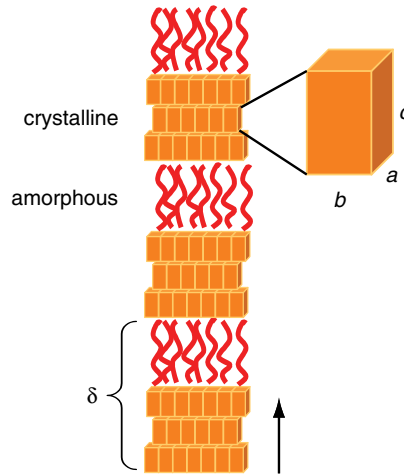


Fig. 7 Molecular semi-crystalline PEEK film model. The parameter δ describes the alternating crystalline/amorphous long-range order stacks with a periodicity of 14.66 nm. One crystalline subunit consists of a unit cell with the axes a , b , and c . The semi-crystalline/amorphous repeats are oriented along the machine direction.

cell of PEEK is orthorhombic ($a = 0.775$ nm, $b = 0.589$ nm, and $c = 0.988$ nm)^{14,15} comprising two chains aligned in direction of the c -axis, one chain positioned at the center of the ab -projection and four chains at the corners. The observed WAXS signals at q -values of 8.0 nm⁻¹ and 10.7 nm⁻¹ corresponding to 0.79 and 0.59 nm, respectively, are in reasonable agreement (less than 2% difference) with the a - and b -lattice constants reported. The pronounced ring at 4.0 nm⁻¹, which corresponds to a periodicity of 1.56 nm, however, does not agree with a single lattice constant but may originate from two times a . Figure 4 shows an I - q -plot of the integrated WAXS data of a 25 μm -thin APTIV™ 1000 PEEK film and a 50 μm -thin APTIV™ 2000 PEEK film that was annealed at a temperature of 160°C for a period of 10 min.

The diffraction ring corresponding to anisotropic long-range ordering of 14.66 nm was measured with higher angular resolution in SAXS geometry. A SAXS pattern of an originally amorphous 50 μm -thin PEEK film annealed at 160°C for a period of 10 min is shown in Fig. 5. The main orientation of the scattering signal, and thus of the long-range order, is parallel to the machine direction, fitting the orientation found in the optical measurements. Therefore, one may assume the same source of anisotropy is detected with the two methods. The intensity of the anisotropic scattering signal increased with film thickness from 12 via 25 to 50 μm (see Fig. 6).

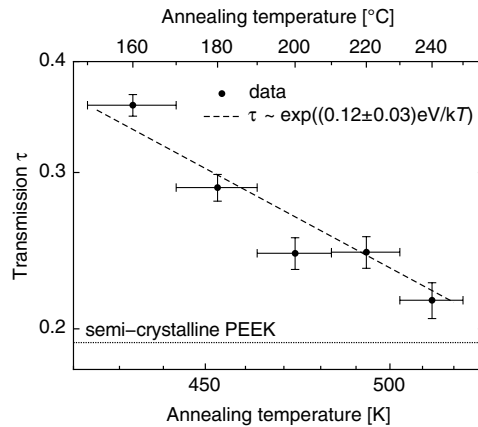


Fig. 8 The Arrhenius-plot of the optical transmission of 50 μm APTIV™ 2000 PEEK films at 540 nm shows the growth of crystallites with a long-range order and a related activation barrier of (0.12 ± 0.03) eV associated with intermolecular interactions.

While the APTIV™ 1000 PEEK films and annealed films exhibited an anisotropic signal, the untreated APTIV™ 2000 PEEK films (reference) were isotropic. This indicates that the anisotropy of the film arises from the bulk of the PEEK films.

3.3 Nanostructure of Semi-Crystalline PEEK Films

The following model, which is known from polymers^{16–18} and is in agreement with the optical and x-ray measurements, is represented in Fig. 7. The long-range order with a periodicity of 14.66 nm describes the amorphous/semi-crystalline long period δ . The unit cell parameter c of PEEK is parallel to machine direction. The long period is oriented in the c -axis direction, and the related q -peak intensities are therefore film thickness dependent.

4 Discussion and Conclusions

The description of semi-crystalline PEEK by means of stacked long-range ordered amorphous and crystalline units agrees with previously published results. Lovinger et al.¹⁹ studied PEEK crystallization from solution and melt, and concluded that both routes produce spherulites with narrow, elongated lamellae, that radially grow in the crystallographic b -axis direction. In this structure, the c -axis lies parallel to the spherulite plane and the a -axis lies vertical to the plane. The interpretation of SAXS data, concerning the lamellar structure is, however, a more difficult task and subject of debates (see Ref. 16 and references therein). Two main models were discussed. In a three-phase model, thick lamellar crystals (7 to 12 nm) separated by thinner amorphous interlayers (3 to 4 nm) pack into stacks of finite size. Extended purely amorphous PEEK regions lie between these stacks. A two-phase model suggests stacks of thin lamellae alternating with thicker amorphous interlayers.¹⁶ The size range of one repeating unit consisting of a crystalline and an amorphous layer is in reasonable agreement with the obtained periodicity of 14.66 nm. Also, the orientation of the lamellae perpendicular to the ab -projection plane fits well to the assumption that the orientation measured in optical transmission and WAXS/SAXS originates from the lamellar stacks.

DSC thermograms of PEEK 2000 films (data not shown) exhibited a pronounced re-crystallization peak around 170°C. This is a common phenomenon observed for polymers that have been cooled down rapidly during processing, thus kinetically preventing crystallization (prominent examples are polyethylene terephthalate and polylactic acid) despite molecular chains being oriented. The present pre-orientation of molecular strands in the amorphous film, upon heating above T_g , facilitates re-crystallization as the molecular motions are deliberated. We suggest that the pre-orientation of the molecules in the 2000 APTIV™ PEEK film, induced by the production process, becomes detectable upon crystallization. This annealing process can be monitored using optical transition measurements as evidenced in Fig. 8. The transmission at a wavelength of 540 nm exhibits the Arrhenius behavior with an activation energy of (0.12 ± 0.03) eV. Similar to organic systems on surfaces²⁰ this value is associated with the intermolecular bond strength within PEEK. For benzene dimers, the π - π binding energy is reported to be in the range of 2 to 3 kcal mol⁻¹,²¹ which corresponds to 0.09 to 0.13 eV per molecule, and therefore reasonably agrees with the activation energy obtained from the Arrhenius plot. Note that for the three-dimensional epitaxial growth of para-hexaphenyl the activation energy corresponds to (0.90 ± 0.04) eV,²² a value which has to be divided by six to deduce the π - π binding energy, and thus it is in agreement with the activation energy derived from the rather simple transmission measurements of annealed PEEK films. One may, therefore, deduce the scenario for the optical measurements on PEEK films. First, amorphous PEEK films are transparent and do not show any anisotropy, because the nanostructures are well below the wavelength of the probe. Second, annealing results in the formation of crystallites within the amorphous matrix, which show a long-range order according to the film processing direction and hence reduce the optical transmission of the PEEK films until the semi-crystalline state has been reached. Both methods, x-ray scattering and optical characterization, sensitive to different length scales, revealed a process-induced anisotropy in PEEK films.

Anisotropic polymer films with a preferential orientation on different lengths are promising materials for medical implants, as most human tissues also show anisotropic structure and properties.¹⁰ In order to realize nature-analogue and biomimetic polymer implants, rather simple optical transmission or reflection measurements could become a vital tool to optimize the structural anisotropy on the nanometer scale.

Acknowledgments

The SAXS experiments were performed on the cSAXS beamline at the Swiss Light Source, Paul Scherrer Institut, Villigen, Switzerland. The support of Teemu Ikonen and Xavier Donath is gratefully acknowledged. We also thank Stefan Stutz for the technical setup and support regarding the optical measurements. This work was funded by the Swiss Nanoscience Institute (project 6.2).

J.A., O.B., H.D., and B.M. have designed the study. J.A. recorded the optical data and prepared the related figures. J.A. and H.D. acquired the x-ray scattering data. All authors significantly contributed to data analysis and interpretation as well as approved the final version of the submitted manuscript. B.M. is the guarantor of integrity of the entire study.

References

1. M. Escuti, D. Cairns, and G. Crawford, "Optical-strain characteristics of anisotropic polymer films fabricated from a liquid crystal diacrylate," *J. Appl. Phys.* **95**(5), 2386–2390 (2004), <http://dx.doi.org/10.1063/1.1643192>.
2. K. Kirov and H. Assender, "Quantitative ATR-IR analysis of anisotropic polymer films: extraction of optical constants," *Macromolecules* **37**(3), 894–904 (2004), <http://dx.doi.org/10.1021/ma030369j>.
3. T. Shimo and M. Nagasawa, "Stress and birefringence relaxations of noncrystalline linear polymer," *Macromolecules* **25**(19), 5026–5029 (1992), <http://dx.doi.org/10.1021/ma00045a032>.
4. I. Ward, *Structure and Properties of Oriented Polymers*, Applied Science, London (1975).
5. X. Zhang et al., "Oriented structure and anisotropy properties of polymer blown films: HDPE, LLDE and LDPE," *Polymer* **45**(1), 217–229 (2004), <http://dx.doi.org/10.1016/j.polymer.2003.10.057>.
6. S. Shoji et al., "Optical polarizer made of uniaxially aligned short single-wall carbon nanotubes embedded in a polymer film," *Phys. Rev. B* **77**(15), 153407 (2008), <http://dx.doi.org/10.1103/PhysRevB.77.153407>.
7. S. M. Kurtz and J. N. Devine, "PEEK biomaterials in trauma, orthopedic, and spinal implants," *Biomaterials* **28**, 4845–4869 (2007), <http://dx.doi.org/10.1016/j.biomaterials.2007.07.013>.
8. "Protecting batteries in heart pacemakers," *Kunststoffe* **2**, 98 (2011).
9. J. Althaus et al., "Nanostructuring polyetheretherketone for medical implants," *Eur. J. Nanomed.* **4**(1), 7–15 (2012), <http://dx.doi.org/10.1515/ejnm-2011-0001>.
10. B. Müller et al., "Scanning x-ray scattering: evaluating the nanostructure of human tissues," *Eur. J. Nanomed.* **3**(1), 30–33 (2010), <http://dx.doi.org/10.1515/EJNM.2010.3.1.30>.
11. O. Bunk et al., "Multimodal x-ray scatter imaging," *New J. Phys.* **11**(12), 123016 (2009), <http://dx.doi.org/10.1088/1367-2630/11/12/123016>.
12. B. Heinrich et al., "PILATUS: a single photon counting pixel detector for x-ray applications," *Nucl. Instrum. Methods* **607**(1), 247–249 (2009), <http://dx.doi.org/10.1016/j.nima.2009.03.200>.
13. A. Rodger and B. Nordén, *Circular Dichroism and Linear Dichroism*, Oxford University Press, Oxford and New York (1997).
14. P. C. Dawson and D. J. Blundell, "X-ray data for poly(aryl ether ketones)," *Polymer* **21**(5), 577–578 (1980), [http://dx.doi.org/10.1016/0032-3861\(80\)90228-1](http://dx.doi.org/10.1016/0032-3861(80)90228-1).
15. J. N. Hay et al., "The structure of crystalline PEEK," *Polym. Commun.* **25**(6), 175–178 (1984).

16. G. Reiter and J.-U. Sommer, "Polymer crystallization: observations, concepts and interpretations," *Lect. Notes Phys.* **606**, 1–382 (2003), <http://dx.doi.org/10.1007/3-540-45851-4>.
17. J. I. Lauritzen and J. D. Hoffman, "Theory of formation of polymer crystals with folded chains in dilute solution," *J. Res. Nat. Bur. Stand.* **64A**(1), 73–102 (1960).
18. A. Ryan et al., "A synchrotron x-ray study of melting and recrystallization in isotactic polypropylene," *Polymer* **38**(4), 759–768 (1997), [http://dx.doi.org/10.1016/S0032-3861\(96\)00583-6](http://dx.doi.org/10.1016/S0032-3861(96)00583-6).
19. A. J. Lovinger and D. D. Davis, "Solution crystallization of poly(ether ether ketone)," *Macromolecules* **19**(7), 1861–1867 (1986), <http://dx.doi.org/10.1021/ma00161a014>.
20. B. Müller, "Natural formation of nanostructures: from fundamentals in metal heteroepitaxy to applications in optics and biomaterials science," *Surf. Rev. Lett.* **8**(1–2), 169–228 (2001), [http://dx.doi.org/10.1016/S0218-625X\(01\)00085-9](http://dx.doi.org/10.1016/S0218-625X(01)00085-9).
21. M. Sinnokrot, E. Valeev, and C. Sherrill, "Estimates of the ab initio limit for π - π interactions: the benzene dimer," *J. Am. Chem. Soc.* **124**(36), 10887–10893 (2002), <http://dx.doi.org/10.1021/ja025896h>.
22. B. Müller et al., "MBE growth of para-hexaphenyl on GaAs(001)-2 \times 4," *Surf. Sci.* **418**(1), 256–266 (1998), [http://dx.doi.org/10.1016/S0039-6028\(98\)00720-1](http://dx.doi.org/10.1016/S0039-6028(98)00720-1).



Jasmin Althaus received a diploma in chemistry from the University of Applied Sciences, Northwestern, Switzerland, in 2004. After working at the Friedrich Miescher Institute in Basel as a research assistant with Jan Hofsteenge, she moved on to the Biocenter in Basel, where she earned a molecular biology MSc in 2008. She is currently working towards her PhD degree in biomedical engineering on the effect of plasma-treated PEEK films on human mesenchymal stem cell differentiation at University of Basel, University of Rostock, Paul Scherrer Institute and University of Applied Sciences, and Arts Northwestern Switzerland with the aim to

obtain the degree from the medical faculties of the universities in Basel and Rostock.



Hans Deyhle received a MSc diploma in experimental physics from ETH, Zurich, in 2008. He has worked as scientist and later as PhD student in the team of Bert Müller at the Biomaterials Science Center of the University of Basel. He is mainly dealing with micro- and nano-imaging of human teeth using x-rays from synchrotron radiation sources in Villigen/Switzerland, Hamburg/Germany, and Grenoble/France.



Oliver Bunk received a PhD in physics from the University of Hamburg. He is currently heading the laboratory for macromolecules and bioimaging of the Swiss Light Source at the Paul Scherrer Institute. Recurrent themes of his research include cross-disciplinary work using x-ray techniques, which he has developed towards perfection step-wise. The current focus relates to bioimaging of hierarchically structured materials using scanning small-angle x-ray scattering and coherent diffractive imaging.



Per Magnus Kristiansen received a MSc diploma in materials sciences from the ETH, Zurich, in 2000. He then joined the polymer technology group of Paul Smith at ETH, Zürich for a PhD project on nucleation and clarification of semi-crystalline polymers. In 2004 he started to conduct applied research on functional supramolecular additives at Ciba. From 2007 to 2009 he was responsible for customer support for light stabilizers, functional additives, and nanoparticles. In 2009 he became a professor at the Institutes of Polymer Engineering and Polymer Nanotechnology. He deals with micro- and nano-structuring by injection molding, nanoimprint

lithography, roll embossing, and microthermoforming.



Bert Müller received a MSc degree in physics from the Dresden University of Technology and a PhD in physics from the University of Hannover, Germany, in 1989 and 1994, respectively. From 1994 to 2001, he worked as a researcher at the Paderborn University, Germany, and subsequently in Switzerland at EPF Lausanne, and ETH Zurich. He became a faculty member of the Physics Department at ETH, Zurich, in 2001. After his election as Thomas Straumann-Chair for Materials Science in Medicine at the University of Basel, Switzerland and his appointment at the Surgery Department of the University Hospital Basel in 2006, he founded the Biomaterials Science Center. He teaches physics and materials science at the Universities of Basel and Bern as well as at ETH, Zurich. He is a member of SPIE and Associate Editor of the *Journal of Nanophotonics*.